AD-A140 832 PROCESSING AND PROPERTIES OF AIRFRAME MATERIALS(U) 1/1
ROCKWELL INTERNATIONAL THOUSAND OAKS CA SCIENCE CENTER
J A WERT ET AL. FEB 84 SC5358.2AR AFOSR-TR-84-0250
UNCLASSIFIED F49620-83-C-0055 F/G 11/6 NL

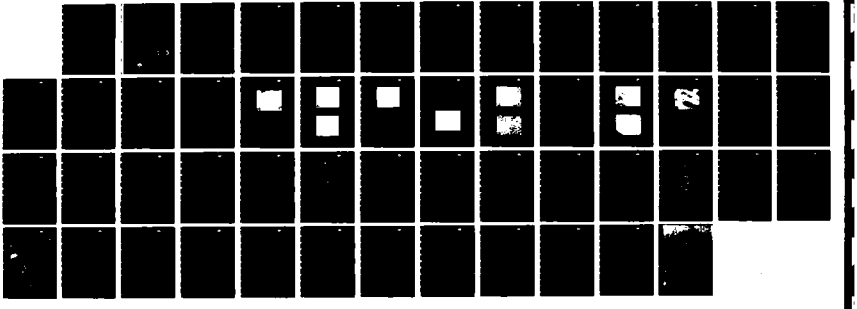

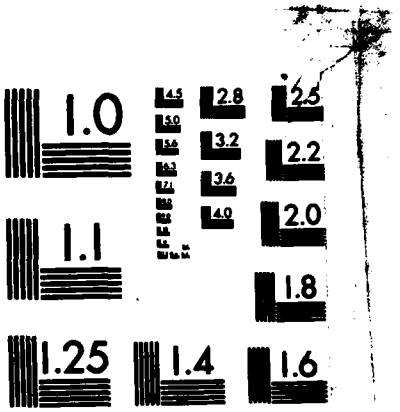

3

SC5358.2AR

SC5358.2AR

Copy No. 5

PROCESSING AND PROPERTIES OF AIRFRAME MATERIALS

ANNUAL REPORT FOR THE PERIOD
January 1, 1983 through December 31, 1983

CONTRACT NO. F49620-83-C-0055

Prepared for

Air Force Office of Scientific Research
Directorate of Electronic and Materials Sciences
Building 410
Bolling Air Force Base, DC 20332

PART I
J.A. Wert, J.C. Chesnutt, C.G. Rhodes

PART II
A.K. Ghosh

FEBRUARY 1984

Approved for public release; distribution unlimited

Rockwell International
Science Center

8a. NAME OF FUNDING/SPONSORING ORGANIZATION	8b. OFFICE SYMBOL (If applicable)	9. PROCUREMENT INSTRUMENT IDENTIFICATION NUMBER
Air Force Office of Scientific Research	NE	Contract No. F49620-83-C-0055

8c. ADDRESS (City, State and ZIP Code)	10. SOURCE OF FUNDING NOS.			
Building 410 Bolling Air Force Base, DC 20332	PROGRAM ELEMENT NO.	PROJECT NO.	TASK NO.	WORK UNIT NO.
	61102F	2306/A1		

11. TITLE (Include Security Classification)
PROCESSING AND PROPERTIES OF AIRFRAME MATERIALS (U)

12. PERSONAL AUTHOR(S)
Wert, John A.; Ghosh, Amit K., Chesnutt, James C.; Rhodes, Cecil G.

13a. TYPE OF REPORT	13b. TIME COVERED	14. DATE OF REPORT (Yr., Mo., Day)	15. PAGE COUNT
Annual Report	FROM 01/01/83 TO 12/31/83	FEBRUARY 1984	50

16. SUPPLEMENTARY NOTATION

17. COSATI CODES			18. SUBJECT TERMS (Continue on reverse if necessary and identify by block number)
FIELD	GROUP	SUB. GR.	Metals Processing, Titanium, Aluminum, Fatigue, Superplasticity.

TABLE OF CONTENTS

LIST OF FIGURES

LIST OF FIGURES

1.0 ABSTRACT

This annual report describes progress during the first year of the three year research program to study the relationship between microstructure and processing conditions, and the effect of processing conditions on the performance of structural airframe materials. Part I of this program is examining the influence of beta processing methods on the interaction of fatigue cracks with the microstructural elements. Three beta phase processing methods have been chosen to provide variations in beta phase continuity and alpha phase plate size. The microstructure of the beta processed materials has been quantitatively characterized using SEM, TEM and STEM. Fatigue crack propagation results are also presented for each of the beta annealing treatments.

In Part II, the micromechanics of superplastic deformation are being studied to determine how the microstructural variables affect the macroscopic deformation behavior. Experiments have been performed with 7475 Al having various grain sizes. The flow stress vs strain rate behavior for the mixed grain size materials is best described using the iso-strain rate concept. Observations of dynamic grain growth and dynamic recrystallization have led to new perceptions of how these processes may alter the mechanical response of the materials during superplastic deformation. Based on these observations, the new model of the superplastic deformation process is outlined.

2.0 INTRODUCTION

Structural properties of airframe materials depend on the processing methods used for component fabrication. The processing methods can either be separate heat treatments designed to produce specific properties, or they can be fabrication steps, such as forging or forming operations. This annual report describes progress during the first year of a three year program to investigate two important aspects of processing of airframe materials.

The overall objectives of this two-part program are to understand the relationship between microstructure and processing conditions, and how the processing conditions influence the performance of structural airframe materials. In Part I of this program, microstructural characteristics of beta processed titanium aloys are being correlated with the fracture path through the microstructure and with tensile and fatigue properties. In Part II of the program, several mechanistic aspects of superplastic forming of high strength aluminum alloys are under investigation to aid in understanding the importance of grain size and grain size distribution on superplastic forming of I/M and P/M Al alloys.

Beta processed Ti alloys, investigated in Part I of this program, can display attractive combinations of strength and fatigue crack propagation (FCP) resistance. However, beta processed alloys have not been used extensively for airframe applications. The microstructures of beta processed Ti alloys are not well characterized compared with conventional alpha-beta processed alloys. Furthermore, a wide range of fatigue crack propagation rates are often found for similar beta processing routes. This program is designed to enhance our understanding of the relationship between processing, microstructure, and FCP properties of beta processed Ti alloys.

In Part I, several beta processing routes for Ti-6Al-4V are being investigated. The effect of these processing steps on the microstructure are being carefully characterized to understand the effect of the processing method on features such as phase morphology, phase composition, and continuity

of the retained beta phase. The effect of the processing method on FCP properties is also being studied to correlate with the microstructural results. In the second year of the program, the paths that fatigue cracks follow through the various microstructures will be determined. Combination of these results will lead to an understanding of how the various microstructural features control fatigue crack propagation, and will allow selection of beta processing routes that provide attractive property combinations for airframe components designed to damage tolerant specifications.

Part II of this program is concerned with superplastic forming of metals. The value of superplastic forming (SPF) as a cost-effective method of fabricating structurally efficient aerospace components is becoming increasingly apparent.[1-3] Significant cost and weight reductions have been demonstrated over conventional fabrication methods. While this technology is reasonably well developed for Ti alloys, high strength Al alloys provide a potentially larger application of SPF technology. This is because of the very widespread use of aluminum in aircraft, spacecraft and missile applications.

A processing method has been developed at the Rockwell International Science Center to impart superplasticity to 7475 Al which has demonstrated the capability of being formed into complex structural components.[3] The primary development has been a thermomechanical processing method for grain refinement, which provides the fine grain size necessary for superplasticity. Aspects of the grain refinement process and its effect on service properties of 7075 Al have been previously investigated under AFOSR sponsorship.[4] However, development of superplastic aluminum is at a relatively early stage, and the importance of various microstructural features such as grain size distribution are not yet understood. Furthermore, much emphasis is currently being placed on P/M Al alloys that offer high strength levels. Development of superplasticity in these alloys would provide benefits from both high strength and improved formability.

In Part II, with an aim of developing an understanding of the role of key microstructural variables on superplasticity of single phase materials,

critical experiments were made during the final year to assess the roles of grain size distribution, dynamic grain growth, and dynamic recrystallization effects during superplastic flow in a fine grain 7475 Al alloy. Model material, fabricated by mixing a specific fine and coarse grain combination, has shown that stress-strain rate characteristics, m values, and stress vs strain curves are intermediate between the data for the individual grain size materials. The composite data are best described by an iso-strain rate assumption applied on the constituent fine and coarse grains. Studies on microstructural changes indicated that dynamic grain growth, although significantly more rapid than static growth, is relatively sensitive to applied strain rate. The distribution of grain size, including the median size, moves to larger sizes with increasing superplastic deformation, thus suggesting that smaller grains do not shrink in size prior to their disappearance. While dynamic growth is most common for the finer grains and slower strain rates, the coarser grains and higher strain rates give rise to concurrent grain refinement (i.e., dynamic recrystallization). Based on these observations, a model has been developed that incorporates 1) the gradual development of dislocation structure, 2) enhancement of diffusional creep rates with increasing grain deformation rate, and 3) dynamic grain growth. Further developments of the model will continue in the second year of the program.

3.0 PROGRESS

3.1 Abstract of Progress

During the first year of this research program, progress has been made on both parts of the program. The results are summarized in the following paragraphs.

Part I - Three beta annealing procedures have been selected for processing the Ti-6Al-4V alloy being used in this investigation. The processes were selected to vary the continuity of the retained beta phase and the alpha plate size. These microstructural elements have been shown to affect fracture properties in previous programs. Quantitative metallography has been performed to establish the volume fraction of beta phase, the beta phase discontinuity density, the alpha plate size and the alpha plate aspect ratio. Large variations in alpha plate size and beta phase discontinuity density were achieved through the processing variations. In addition, the compositions of the alpha and beta phases were determined using STEM methods. Little variation in alpha phase composition was found, but higher annealing temperatures and slower cooling rates caused larger amounts of V and smaller amounts of Al to be present in the beta phase. Fatigue crack propagation properties were measured for the three beta processing methods. Only small differences were found in fatigue crack propagation properties for the three beta annealing procedures. However, different fatigue crack propagation properties were obtained for the load decreasing and load increasing portions of the tests. It is felt that this may be a microstructural effect, and work is underway to confirm this idea.

Part II - With the aim of developing an understanding of the role of key microstructural variables on superplasticity of single phase materials, critical experiments were carried out to assess the roles of grain size distribution, dynamic grain growth and dynamic recrystallization effects during superplastic flow in a fine grain 7475 Al alloy. Model material, fabricated by mixing a specific fine and coarse grain combination, has shown that stress-

strain rate characteristics, m values, and stress vs strain curves are intermediate between the data for the individual grain size materials. The composite data are best described by an iso-strain rate assumption applied to the constituent fine and coarse grains. Studies on microstructural changes indicated that dynamic grain growth, although significantly more rapid than static growth, is not highly sensitive to applied strain rate. The distribution of grain size, including the median size, moves to larger sizes with increasing superplastic deformation, thus suggesting that smaller grains do not shrink in size prior to their disappearance. While dynamic grain growth is common for the smaller grains and slower strain rates, the coarser grains and higher strain rates give rise to concurrent grain refinement via dynamic recrystallization.

3.2 Part I. Effect of Processing on Microstructure and Design Properties of Ti Airframe Alloys

This section describes progress made on Part I during the first year of the three-year program to characterize the relationship between microstructure and fatigue behavior of beta processed Ti-6Al-4V. The program goals are described, followed by a short discussion of previous work on beta processed Ti alloys. Progress in several areas of Part I of this program is then detailed.

3.2.1 Program Goals

The overall objectives of Part I of this three-year program are:

1. To quantitatively characterize the microstructure of beta processed Ti-6Al-4V.

2. To evaluate the path that fatigue cracks follow through the microstructure in beta processed Ti-6Al-4V.

3. To measure the fatigue crack propagation properties of beta processed Ti-6Al-4V.

4. Using the results of microstructural characterization, fatigue properties and fatigue crack path evaluation; to understand how microstructural features of beta processed Ti alloys affect fatigue properties.

In the first year, substantial progress has been made toward these ultimate goals. Studies have concentrated on characterization of the microstructures and fatigue properties of Ti-6Al-4V produced by three different beta processing methods. For these selected processing methods, goals 1 and 3 listed above have been achieved. Current efforts to establish the relation-

ship between microstructure and crack path address goal 2, and correlation of these results (goal 4) will meet the overall program objective.

3.2.2 Background

Current and future generation high performance aircraft are being designed with alloys that have high specific strength levels. Current design philosophies utilize the Air Force structural integrity philosophy, as described in military standard MIL-STD-1530A, Aircraft Structural Integrity Program, Airplane Requirements. Inherent in this design philosophy is a requirement for resistance to fatigue crack propagation. This emphasis on damage tolerant design and fatigue crack propagation resistant materials has led to consideration of beta processed Ti alloys for fracture-critical applications. The titanium alloy Ti-6Al-4V has been utilized in such fracture critical designs, but requires a special heat treatment, termed recrystallization anneal, to provide adequate toughness and FCP resistance for these applications. Several previous studies of the effect of microstructure on properties of Ti-6Al-4V have demonstrated that the beta processed or beta annealed microstructures offer considerable improvement in FCP resistance. In the context of this program, beta processing refers to microstructures that have been produced by either working above the beta transus, heat treating above the beta transus subsequent to working operations, or a combination of the two.

A significant potential also exists for replacing components which are extensively machined with precision forged Ti alloys. Forging at temperatures above the beta transus, where the flow stress is significantly reduced, would allow production of more complex geometries than are possible by forging below the beta transus.

The effect of processing above the beta transus on microstructure and fatigue crack propagation resistance has not been well characterized. In a study at the Science Center, Rhodes has evaluated the effect of processing below the beta transus on fracture properties of Ti-6Al-4V. His results showed that the fracture properties could be correlated with the distribution and

morphology of the alpha and beta phases, and with the chemical partitioning between the two phases.[5] A second program showed that the distribution and continuity of the retained beta phase affected the fracture toughness of beta processed Ti alloys of various compositions.[6]

Although beta processing can lead to improved fatigue crack propagation resistance in Ti alloys, there is an attendant increase in variation of crack propagation rates compared to alpha-beta processed alloys. It is thought that much of this variability in properties stems from the path that the fatigue cracks follow through the microstructure and their interaction with various microstructural features. Part I of this program seeks the links between microstructure, crack path and FCP properties. The knowledge gained in Part I of this program will enable tailoring of beta processing treatments to provide microstructures with high fatigue crack propagation resistance and smaller variability in properties.

3.2.3 Heat Treatment Selection

The chemical composition of the Ti-6Al-4V alloy used in Part I of the program is shown in Table I. The beta-processed microstructure was developed

Table I

Chemical Composition of Ti-6Al-4V

Element:	Al	V	O	C	N	H	Ti
Wt %:	6.08	3.98	0.124	0.015	0.009	0.0074	Bal.

by annealing above the beta transus, followed by an air cool. The two significant microstructural features that must be considered when Ti alloys are processed in the beta phase field are the beta grain size and grain boundary alpha. Yoder and co-workers[7,8] demonstrated that an increased beta grain size is beneficial for fatigue crack propagation resistance, but detrimental to tensile strength and ductility. In this program, it was decided to select a

beta grain size intermediate to those examined by Yoder et al so that neither the fatigue crack propagation resistance nor the tensile properties would be seriously degraded. The solution treatment selected for these studies was a 10 min exposure at 1025°C (beta transus + 25°C). Grain boundary alpha forms at beta phase grain boundaries during cooling from above the beta transus. The amount of grain boundary alpha present in the microstructure is a function of the cooling rate, with more alpha forming as the cooling rate decreases. However, because thick sections of Ti-6Al-4V used in airframe applications cannot always be cooled rapidly enough to preclude grain boundary alpha, the beta anneal treatment has been followed by an air cool rather than a quench. Although this procedure results in the formation of grain boundary alpha, it will closely simulate the sort of microstructure that will be present in thick sections. Figure 1 illustrates the beta annealed microstructure.

The objective of this program is to study the influence of beta-processed microstructure on fatigue crack propagation. The microstructure of a beta-processed Ti alloy such as Ti-6Al-4V can vary significantly depending upon the type of processing that the alloy undergoes. Those features that may affect fatigue properties are volume fractions and compositions of alpha and beta phases, size of alpha and beta grains, and continuity of beta phase. Heat treatments that follow the beta anneal have been devised to systematically vary these elements of the microstructure so that their effect on fatigue may be evaluated.

The three heat treatments that have been used in this study are listed in Table II. Treatment #1 involves a hold midway in the alpha-beta phase field to generate a moderate amount of discontinuous beta phase, followed by an air cool, which will result in a fairly fine alpha plate size with a high aspect ratio. Treatment #3 includes a very slow cool from just above the beta transus to room temperature to develop a low volume fraction of continuous beta phase and a coarse alpha plate size with a moderate aspect ratio. Treatment #2 is intended to produce microstructures intermediate to those generated by treatments #1 and #3. To achieve this, the alloy is held for a

short time high in the alpha plus beta phase field to provide some coarsening of the preexisting beta phase, followed by a slow cool to develop larger alpha plate size and continuity of the beta phase. Finally, air cooling from a temperature midway in the alpha plus beta phase field essentially retains the alpha-beta mixture attained during the slow cooling step.

Table II
Heat Treatment Schedule to Follow Beta Anneal

Condition No.	Treatment
1	750°C/1 h/air cool
2	925°C/30 min/cool at 60°C per hour to 750°C/air cool
3	1000°C/10 min/cool at 50°C per hour to room temperature

3.2.4 Microstructure Characterization

The beta annealed condition, Fig. 1, has a prior beta grain size of about 350 μm and nearly continuous grain boundary alpha that is approximately 3 μm wide. None of the three post-beta anneal heat treatments significantly alters the prior beta grain size or the amount of grain boundary alpha.

The volume fractions, compositions and dimensions of alpha and beta grains, and continuity of beta phase have been evaluated as a function of heat treatme Table III lists the volume fractions and continuity of beta phase for th t treatments. As anticipated, condition #1 exhibits the largest volume acti of beta phase and a more discontinuous beta phase. Figures 2 through llustrate the relative distributions of beta phase in the three heat treat conditions. Continuity of the beta phase is reported as discontinuities per cubic centimeter of alloy, and is measured by counting the number of terminations of beta strips per area on a polished and etched surface. Clearly, then, a larger number of discontinuities represents a less continuous

Fig. 1 Light micrograph of Ti-6Al-4V after beta treatment of 1025°C/10 min/AC.

Table III

Volume Fraction and Discontinuity of Beta Phase in Ti-6Al-4V

Condition No.	Volume Fraction Beta Phase	Discontinuities of Beta Phase, Per cm^3
1	0.19	6.5×10^{12}
2	0.14	1.9×10^{11}
3	0.10	1.2×10^{11}

Fig. 2 SEM of Ti-6Al-4V given heat treat condition 1. Beta phase is white.

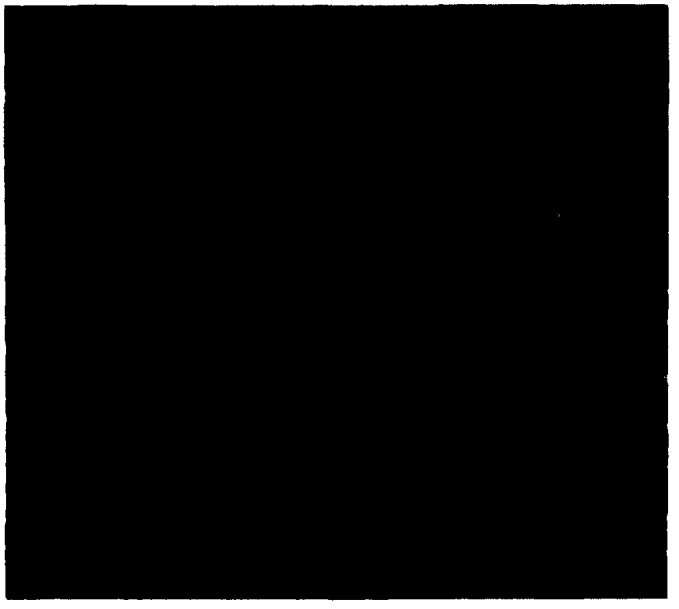

Fig. 3 SEM of Ti-6Al-4V given heat treat condition 2. Beta phase is white.

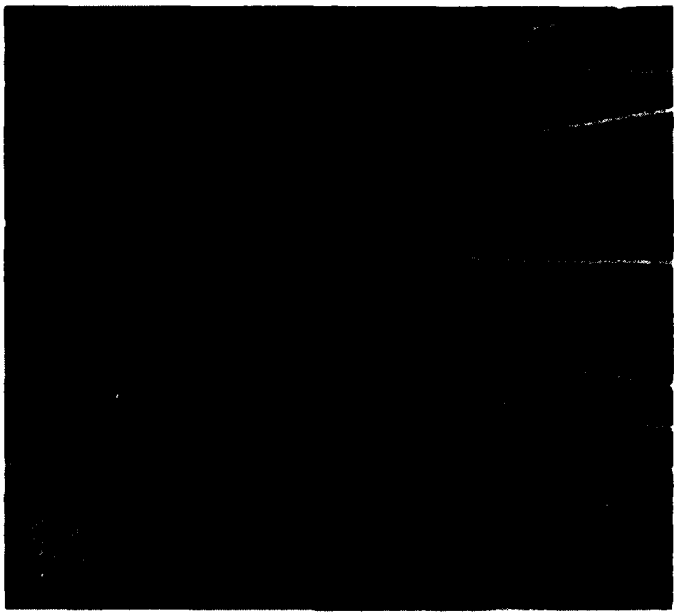

Fig. 4 SEM of Ti-6Al-4V given heat treat condition 3. Beta phase is white.

beta phase. Although the number of discontinuities will be related to the volume fraction of beta phase, there is not a simple one-to-one ratio for the heat treatments utilized in this study. Hence, whether the discontinuities are reported as the absolute values measured (as listed in Table III) or as values normalized to volume fraction beta, heat treatment #1 results in more than an order of magnitude greater number of discontinuities than treatments #2 or #3. The heat treatments have succeeded in varying the volume fraction of beta phase by a factor of two, and beta phase discontinuity by more than an order of magnitude.

The alpha phase parameters are listed in Table IV. Treatment #1 has resulted in the finest alpha plate size and the largest aspect ratio, while Treatment #3, as expected, has produced the largest alpha plate size and the smallest aspect ratio. The microstructures are illustrated in Figs. 5 through 7.

Table IV

Alpha Phase Dimensions in Ti-6Al-4V

Condition No.	Average Length Alpha Phase Plate (μm)	Average Width Alpha Phase Plate (μm)	Alpha Phase Aspect Ratio
1	21	0.9	24:1
2	32	1.8	17:1
3	80	6.0	13:1

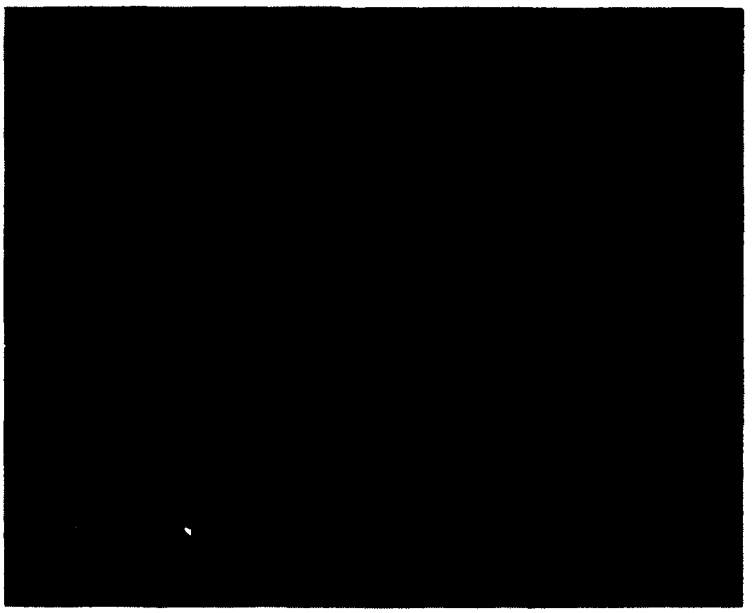

Fig. 5 Light micrograph of Ti-6Al-4V given heat treat condition 1. Alpha phase is light, beta phase is dark.

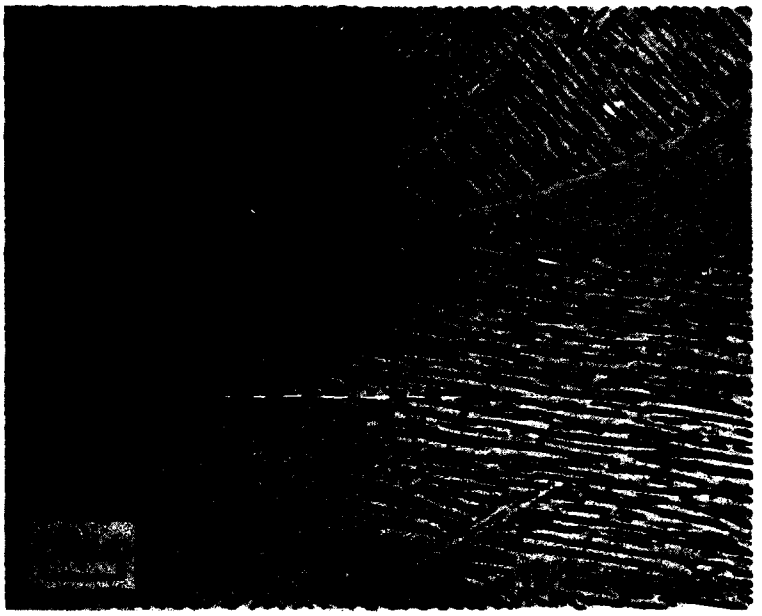

Fig. 6 Light micrograph of Ti-6Al-4V given heat treat condition 2. Alpha phase is light, beta phase is dark.

Fig. 7 Light micrograph of Ti-6Al-4V given heat treat condition 3. Alpha phase is light, beta phase is dark.

The final microstructural parameters analyzed in this program are the compositions of the alpha and beta phases. The chemical analyses have been accomplished by means of thin foil scanning-transmission electron microscopy using a quantitative x-ray energy dispersive spectroscopy technique developed previously.[9] The results, presented in Table V, reveal the degree to which Al partitions to the alpha phase and V to the beta phase. The alpha phase data given in Table V are for the matrix alpha plates, and do not include the grain boundary alpha which would be expected to contain slightly higher Al and lower V contents.[9] Among the the three treatments, the Al and V concentrations in alpha vary only slightly, whereas they vary significantly in the beta phase. These compositional variations are closely related to the volume fractions of the two phases, which vary only by about 10% for the alpha phase (from .81 to .90), but by 90% for the beta phase (from .10 to .19). Typical microstructures are illustrated in Figs. 8 through 10.

Table V

Compositions of Alpha and Beta Phases in Ti-6Al-4V

Condition No.	Alpha Phase		Beta Phase	
	Wt% Al	Wt% V	Wt% Al	Wt% V
1	7.2	1.8	3.5	15.8
2	7.7	1.7	2.1	17.3
3	7.3	1.5	1.7	23.2

The heat treatments selected for use in this program, Table II, have produced the systematic variations in microstructure, Tables III through V, required for analysis of the influence of beta processing on fatigue crack propagation. The individual values of the several microstructural parameters do not vary in the same way with heat treat conditions, e.g., conditions 2 and

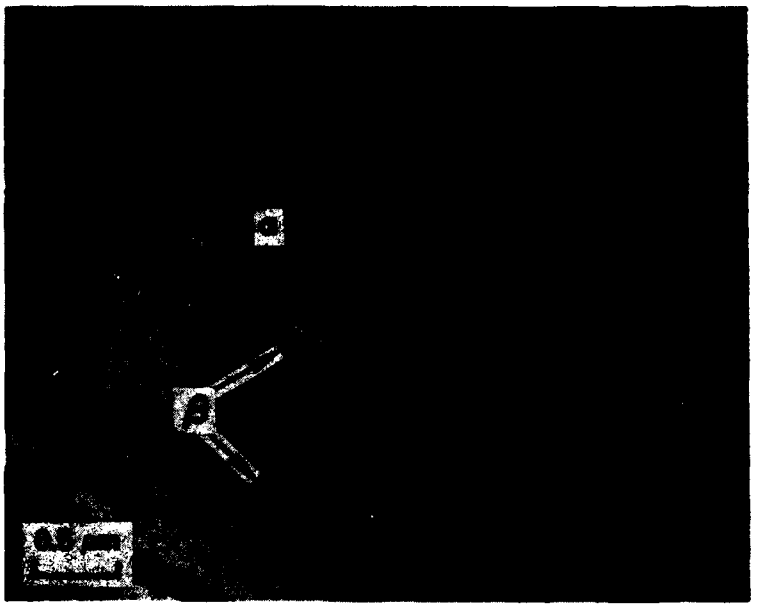

Fig. 8 TEM of Ti-6Al-4V given heat treat condition 1.

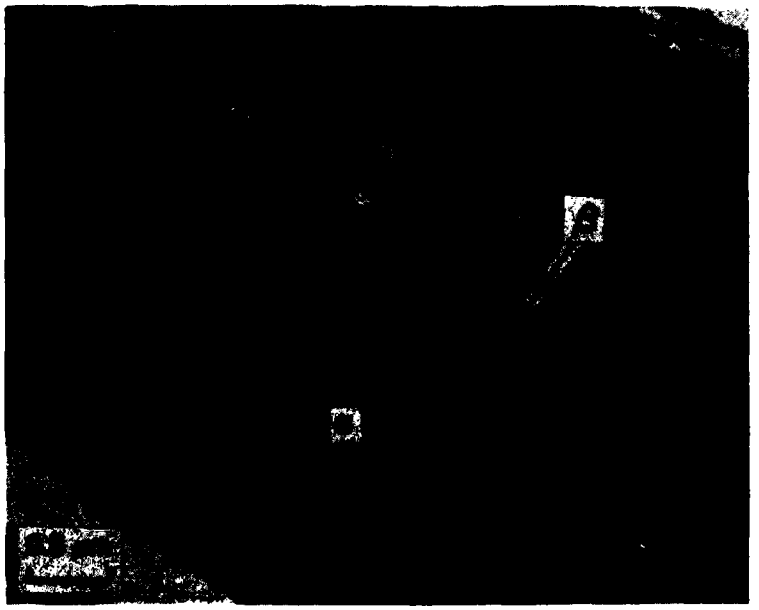

Fig. 9 TEM of Ti-6Al-4V given heat treat condition 2.

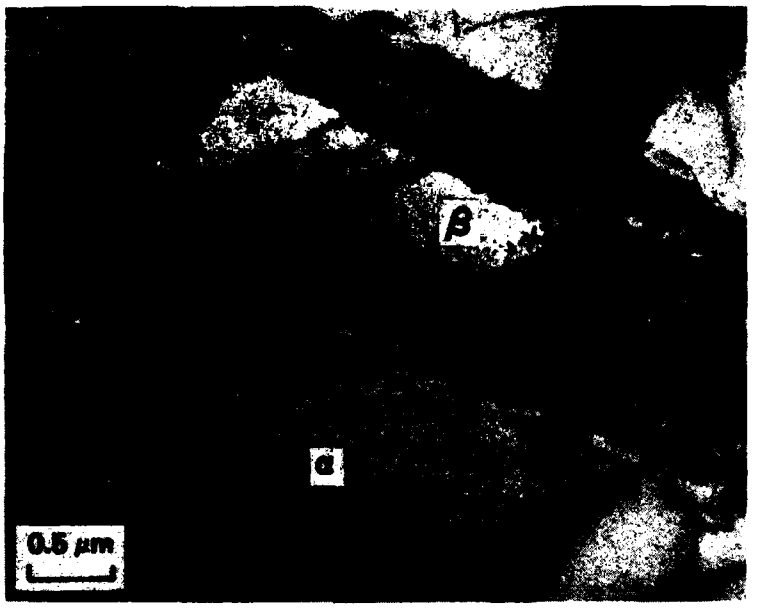

Fig. 10 TEM of Ti-6Al-4V given heat treat condition 3.

3 produce similar values for beta phase discontinuities that are quite different from the value produced by condition 1, whereas conditions 1 and 2 generate similar values for alpha phase plate size compared to the value generated by condition 3. For this reason, testing of the three heat treat conditions will be sufficient to evaluate the influence of individual parameters on fatigue crack propagation rate.

3.2.5 Mechanical Properties

Mechanical property evaluation during the first year consisted of room temperature tensile tests and low load ratio, room temperature fatigue crack propagation (FCP) tests of the three microstructural conditions previously described.

All specimens were machined from a Ti-6Al-4V plate which had been previously purchased to the Rockwell International high fracture toughness specification. Tensile specimen blanks were machined such that the tensile axis was parallel to the long transverse (T) direction. The FCP specimens were machined in the TL orientation.

Tensile tests were conducted in accordance with ASTM E 8 using an Instron test machine with a 90 kN load cell. Specimens with a 6.4 mm diameter by 25.4 mm long gauge length were tested at a strain-rate of 1.67×10^{-4} s^{-1}. Fatigue crack propagation tests were conducted in accordance with the proposed ASTM standard test method[10] using the load shedding technique down to a crack growth rate of approximately 1×10^{-7} mm/cycle. Upon reaching this growth rate, several data points were obtained at constant load. The load was then incrementally increased, with two or three data points being obtained at each load. All other test conditions conformed to ASTM E 647 using a compact type (CT) specimen with B = 12.7 mm and W = 50 mm. Tests were conducted in laboratory air (approximately 50% relative humidity) at a frequency of 30 Hz. Tensile data for the three conditions are given in Table VI.

Table VI

Tensile Properties of Conditions Studied

Condition	$\sigma_{0.2}$ (MPa)	σ_u (MPa)	Elong. (%)*	RA (%)
1	805	867	7.7	20
	773	843	8.3	22
2	737	815	9.7	25
	764	836	9.3	25
3	704	773	10.7	29
	701	771	10.3	29

* 25.4 mm gauge length

Fatigue crack propagation results for the three conditions are shown in Figs. 11, 12 and 13. The results of the test for heat treatment #1 are

plotted in Fig. 11, with the data obtained by load shedding (K-decreasing) indicated as filled symbols. The data obtained by load shedding appears somewhat faster than the data obtained by a constant or increasing load (K-increasing). This behavior has been reported for other alloys,[10] where the K-decreasing data are seen to be on the high side of the data set. In the beta processed microstructures of Ti-6Al-4V, the difference in growth rate between the K-decreasing and K-increasing data may, indeed, result from interaction of the crack tip with the local microstructure. This point will be further clarified by completion of the K-increasing tests for heat treatments #2 and #2, and by precision sectioning and subsequent crack path characterization of the FCP specimens planned for the second year of the program.

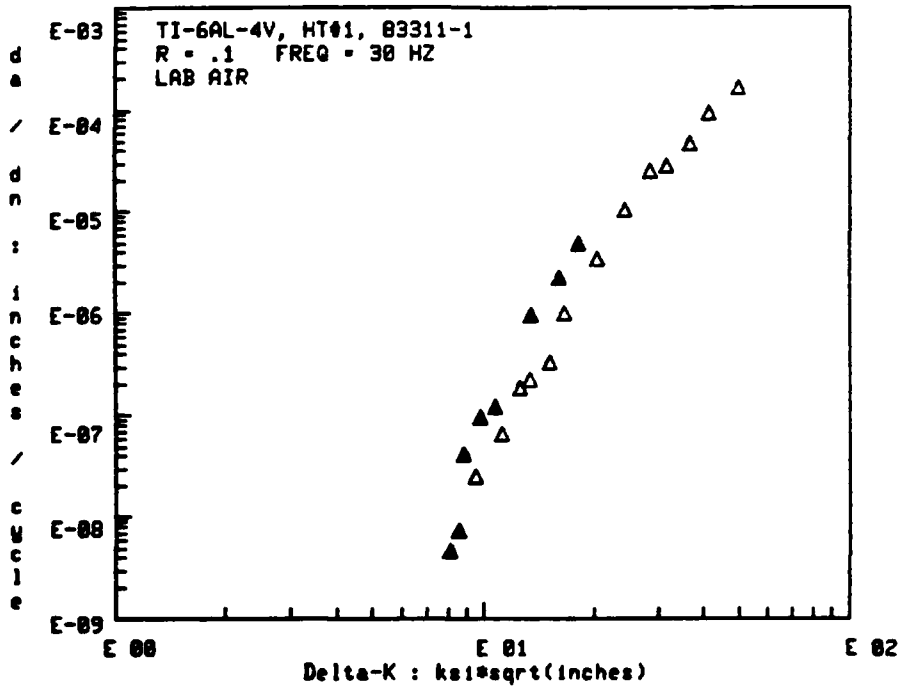

Fig. 11 FCP of Ti-6Al-4V, condition 1, in laboratory air at 30 Hz and R = 0.1. Filled symbols are K-decreasing, open symbols are K-increasing.

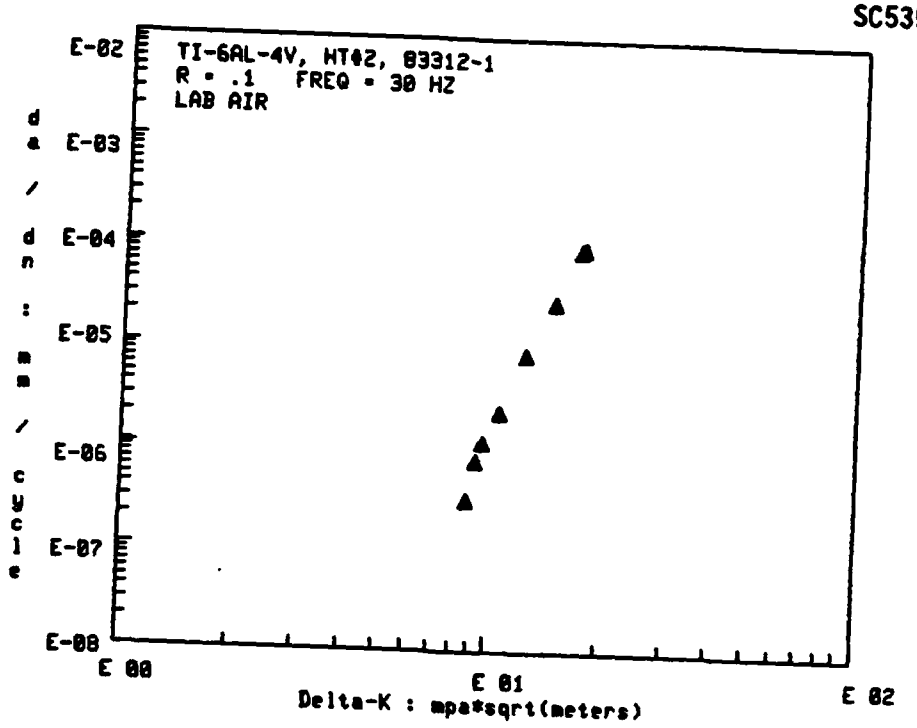

Fig. 12 FCP of Ti-6Al-4V, condition 2, in laboratory air at 30 Hz and R = 0.1. Filled symbols are K-increasing, open symbols are K-increasing.

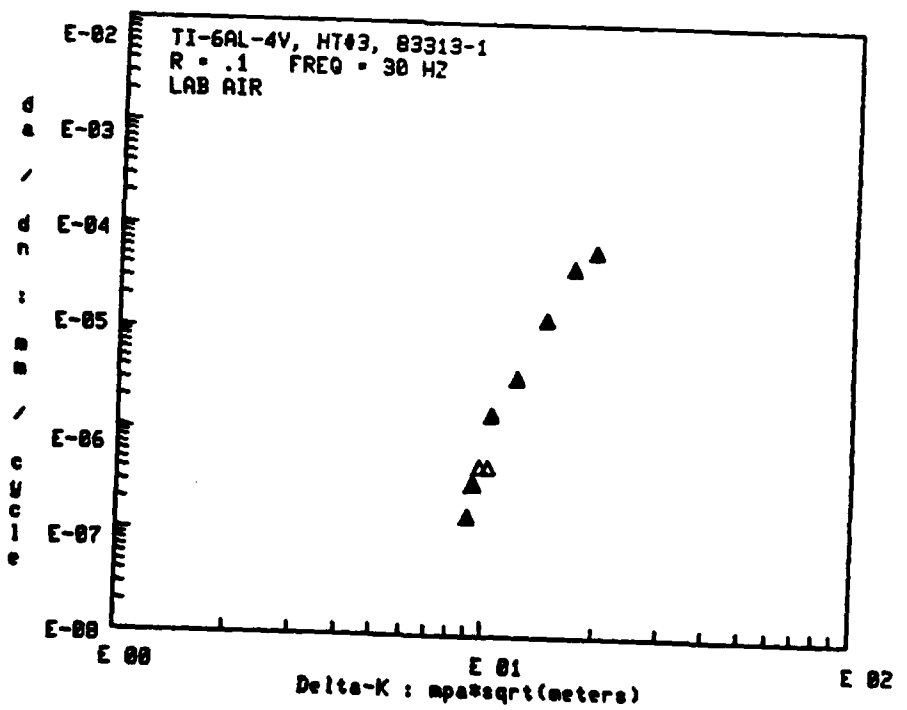

Fig. 13 FCP of Ti-6al-4V, condition 3, in laboratory air at 30 Hz and R = 0.1 Filled symbols are K-decreasing, open symbols are K-increasing.

3.3 Part II. Mechanistic Aspects of Superplasticity in Al Alloys

3.3.1 Background

In spite of the many studies, the understanding of superplasticity mechanisms is far from complete, and it is particularly so for complex alloy systems, e.g., high strength Al alloys. It has been shown recently that grain refinement in conventional high strength Al alloy can lead to its superplastic capability.[3] This offers the potential for significant cost and weight payoff for aerospace structures, and it is likely that this emerging technology will impact the next generation of aircraft by offering this novel capability. While progress continues in the implementation of this technology, since the superplastic flow behavior and the underlying mechanisms of microstructural changes are poorly understood, uncertainties and problems occur periodically during application. A properly focused program to understand and model these effects is essential at this time.

The importance of grain goundary sliding and fine grain size on superplasticity is reasonably well accepted. However, the roles of significant distributions in grains size and microstructural changes occuring during superplastic deformation are poorly understood.[11-13] As a basic point of reference, understanding is lacking as to whether the real behavior of materials follow iso-strain rate or iso-stress models of deformation in various grains. This is of particular importance in designing alloys with improved superplasticity, as well as in determining the optimum processing conditions for their fabrication. The presence of a strong bimodal grain size distribution, as often observed in production heats of Al alloys, may not influence the room temperature service properties in any significant manner, but can drastically alter the superplastic properties. The advent of the RSR powder Al alloys promises significantly higher strength and temperature capabilities in aircraft structures. The knowledge gained on grain size distribution would

be useful for considering appropriate powder particle distributions for improved consolidation and possible superplasticity. If this could be achieved, benefits from both higher strength and improved formability could result.

In all of the mechanistic studies,[14-19] a factor which has been ignored until recently[20,21] is the existence of distributions in grain size. As shown in Ref. 20, while fine grain superplastic metals may have a grain size peak around 5-10 μm, a long tail may exist at much larger grain sizes (~ 30-40 μm). Consequently, any real alloy behaves like a composite material, the fine grains having a different constitutive equation from the coarse grains. Two phase materials (e.g., Ti-6Al-4V, Zn-Al eutectoid, etc.) further possess differences in diffusion coefficients which allow a widely distributed constitutive behavior to be established. It has been possible to show that distributions in metallurgical features such as these could lead to transition from power law to diffusion creep (i.e., region III) which is spread over several decades in strain rate. An assumption which has been tacitly made in such a model is that the same overall strain rate is imposed over a group of fine grains as that over a group of coarse grains. This method provides for the development of internal stress within the material, the coarse grains supporting a higher stress. As opposed to this parallel model, a series model would demand the imposition of iso-stress condition on all grains and allow the strain rates from fine and coarse grains to be added. It appears that experiments designed to test the validity of a parallel or a series model would provide significant insight into the deformation mechanism in a superplastic alloy. Once we can determine how grains of different size slide and interact during superplastic flow, such information will not only provide for an improved model, but a greater opportunity for optimizing microstructure for best superplastic properties.

3.3.2 Objectives

In the first year of this program, the objective for Part II is to determine the effect of certain key microstructural features on the super-

plasticity in Al alloys. Specifically, the influences of grain size, grain size distribution and their changes during superplastic forming are to be assessed and related to the flow and strain induced hardening behavior of these materials. To assess the effect of grain size distribution on superplasticity, model materials with different grain size distributions are to be produced for testing. Characterization of flow stresses and microstructural changes of these materials are to be determined along various orientations to the direction of laminations. The conditions under which an iso-stress or an iso-strain rate criterion for superplastic flow would be operative in a material containing bimodal grain size distributions will be determined. These observations will then be utilized for the development of an overall model for superplastic flow in the second year.

3.3.3 PROGRESS

Progress has been achieved in the following areas:

1. Model material containing a specified mixture of coarse and fine grain microstructures (39:61 by volume) has been fabricated, and superplastic flow behavior has been characterized in several directions of the laminated test material.

2. Microstructural changes of the coarse and fine grain materials during superplastic deformation have been characterized, including dynamic grain growth of the fine grain microstructure and slip band activity and dynamic recrystallization of the coarse grain microstructure.

3. The observations have led to the development of a model for superplastic flow which has the following features: a) enhanced diffusional creep near grain boundaries due to dislocation slip activity, b) enhanced dynamic grain growth due to grain boundary sliding at lower strain rates, and c) dynamic recrystal-

lization and grain subdivision at the higher strain rates. All of these aspects have not been fully developed into a mathematical description as yet, and will be continued as part of the second year program.

3.3.3.1 Model Material Fabrication and Testing

Within this reporting period, a model material was fabricated by lamination of fine and coarse grain 7475 Al alloy sheets (this is a high strength Al alloy containing 5.1% Zn, 2.1% Mg and 1.5% Cu in solid solution, as well as precipitate forming agents and 0.2% Cr as a dispersoid former). The fine grain sheet material was produced by thermomechanical processing from plate 7475 alloy using a patented process[22] which involves overaging the alloy at 400°C for 8 hours after solution treatment (516°C), rolling 90% at 200°C, and subsequently recrystallizing at 516°C. The average grain size of the 2.54 mm thick material so produced was in the neighborhood of 8-12 μm. To produce the coarser grain material, a portion of this sheet was given a 20% rolling reduction at room temperature, followed by a recrystallization treatment at 516°C. This produced grain sizes in the neighborhood of 75 μm. These sheets were thoroughly cleaned, surface abraded, and stacked alternately with fine and coarse grain sheets of 50 mm x 50 mm size to develop a composite with 61% fine grains mixed with 39% coarse grains by volume. The stack was placed inside a stainless steel vacuum bag and press consolidated at 516°C after vacuum outgassing long enough to reach 2×10^{-6} mm Hg in the vacuum gauge. This forge compaction step was carried out in two stages to a total reduction of 8:1 at an overall strain rate of 2×10^{-4} s^{-1} which has previously shown to generate negligible grain growth. The forged block has been sectioned and metallographically evaluated. The microstructures of starting fine and coarse grain materials and the laminated mixed grain size model material are shown in Fig. 14. As expected, the mixed nature of grain size is visible, however, some refinement of microstructure has taken place.

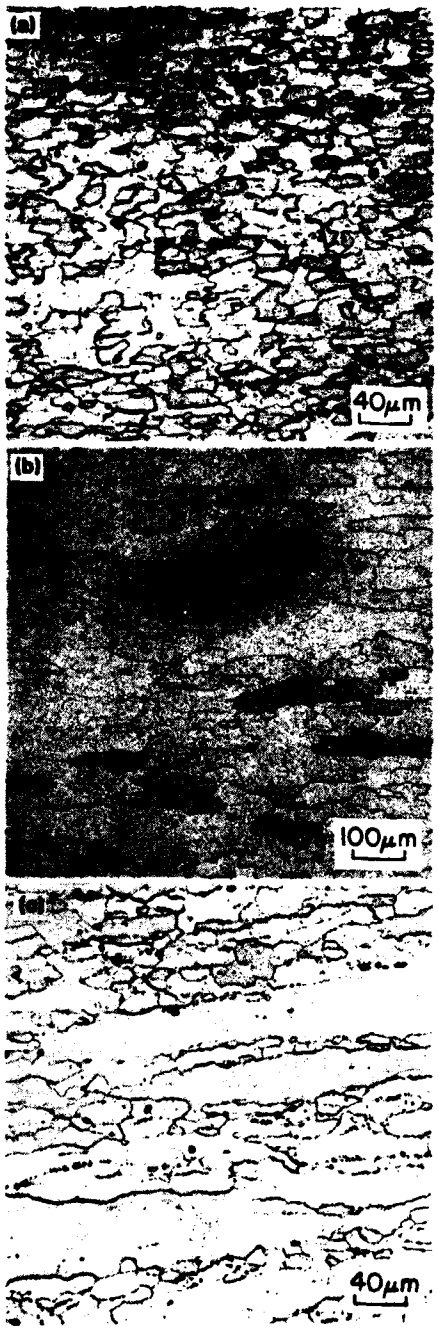

Fig. 14 Grain structures of the constituent fine grain (a), coarse grain (b) materials, and the resultant mixed grain model material (c). All sections in LS plane for 7475 Al. Average grain sizes are respectively 12 μm, 75 μm and 45 μm.

Tensile specimens were machined from the forged block in the plane of laminations (L and T), as well as perpendicular (S) to the lamination planes. Since forging produced a round isotropic pancake, the selection of L and T directions were arbitrary in the plane of forging. The stress vs strain rate plots (from jump test) between the individual directions were not significantly different. However, the S direction had the lowest peak in value (0.60) as compared with 0.75 for the T direction. Figure 15a shows stress vs strain rate data for the fine grain, coarse grain and mixed grain size materials. For the coarse grain material, the results are shown at three different temperatures: 482°C, 516°C and 530°C, the highest temperature producing the most unstable flow. The data for mixed grain size fall between fine and coarse grain results with a slope approaching that of the fine grain Al. Also shown in Fig. 15a are calculated σ-$\dot{\varepsilon}$ plots for mixed grain material obtained from the individual curves for fine and coarse grain materials based on iso-stress and iso-stress rate assumptions. It is clear that iso-strain rate assumption fits the experimental results on the mixed grain (61:39) size material well, except for the very low strain rates. However, because of short transients for coarse grain materials and long transients for fine grain material at the lower strain rates, the calculation of steady state flow stress is biased toward coarse grain size data. Since at low rates the mixed grain size also shows significant transients, the measured stresses are expected to be lower than the steady state values that are calculated. The strain rate sensitivity values (m) determined from the slope of these curves are shown in Fig. 15b. Mixed grain size produced an intermediate value of m between the high of fine grain (m = 0.9) and the low of coarse grain (m = 0.2) materials, with a peak shifted to lower strain rate than that of fine grain materials.

The tensile elongations of all of these test materials are listed in Table VII for a variety of test temperatures and strain rates. Again, the mixed grain size produced intermediate elongation of 360% at 2×10^{-4} s^{-1} (516°C) as compard with 1072% for fine grain and 63% for coarse grain materials. While the S direction had a slightly lower flow stress, it also

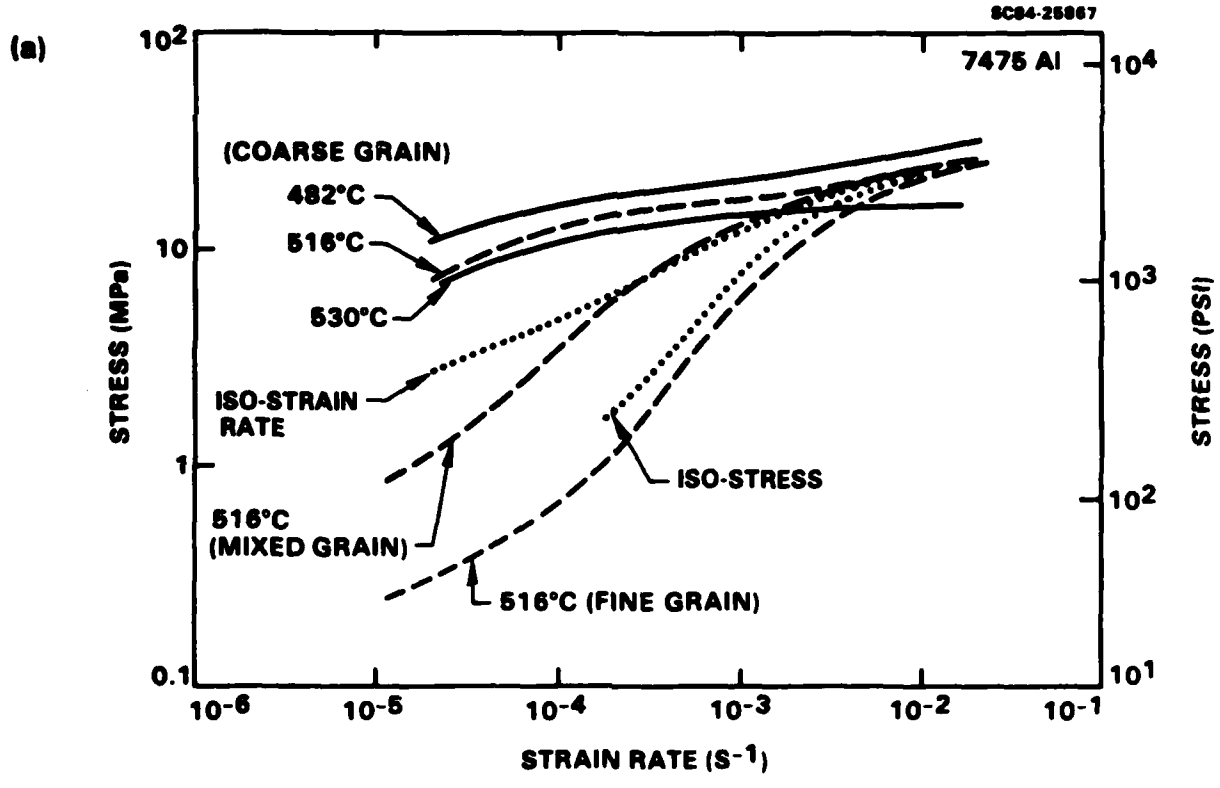

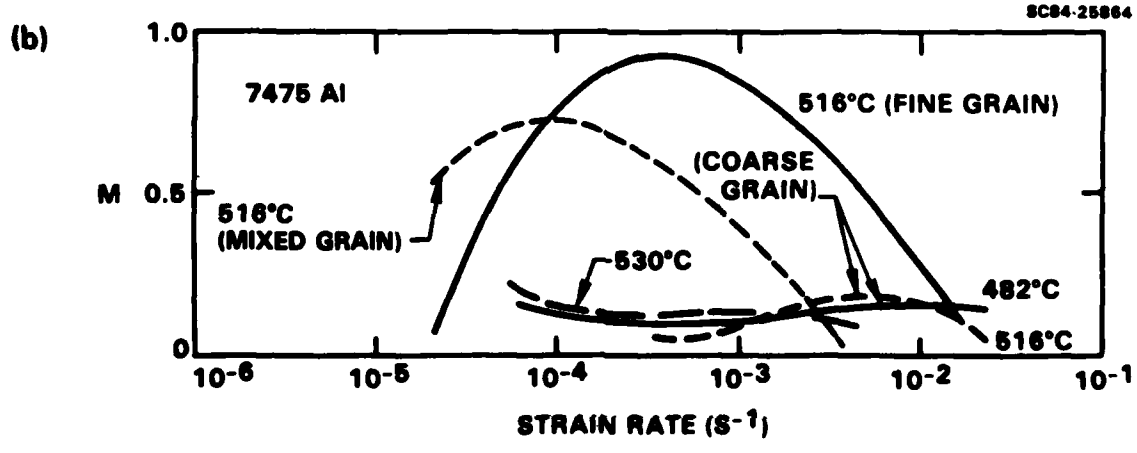

Fig. 15 (a) Stress vs strain rate data from step strain rate test, and (b) m [slope of (a)] vs strain rate for three different grain size conditions.

Table VII

Superplastic Tensile Elongation of the Various Test Materials

Test Temperature	Strain Rate (S^{-1})	Elongation
Coarse Grain 7475 Al		
516°C	10^{-3}	50%
	2×10^{-4}	63%
	5×10^{-5}	99%
530°C	10^{-3}	28%
	2×10^{-4}	15%
482°C	2×10^{-4}	81%
Fine Grain 7475 Al		
	10^{-1}	38%
	10^{-2}	280%
	10^{-3}	540%
516°C	2×10^{-4}	1072%
	10^{-4}	816%
Mixed Grain 7475 Al		
	10^{-3}	251% (L)
		165% (T)
		34% (S)
	2×10^{-4}	360% (L)
		268% (T)
516°C	2×10^{-4}	400% (L)
	(500 psi*)	364% (T)
		122% (S)
		400% (L)
	10^{-4}	292% (T)
		70% (S)

exhibited delamination at oxide layers leading to low elongations. The application of a superimposed hydrostatic pressure,[23] which aids in the suppression of superplastic cavities, was also found to help increase the elongation in the S direction to 122%. The typical σ-ε curves (at constant $\dot{\varepsilon}$) for fine grain, coarse grain and mixed grain materials are shown in Fig. 16 a, b and c. Again, fine grain materials exhibit significant flow hardening at all strain rates, coarse grain materials exhibit flow softening, and mixed grain materials exhibit a period of flow hardening, followed by a flow softening. It is believed that dynamic grain growth, along with a continuous change in the ratio of grain boundary sliding/dislocation creep, is responsible for the flow hardening behavior, whereas strain localization and dynamic recrystallization (grain refinement) of the coarse grains lead to flow softening.

3.3.4 Microstructural Changes

The most important microstructural changes observed during superplastic deformation of 7475 Al are dynamic grain growth at relatively low strain rates and/or fine grain sizes, and dynamic recrystallization (or grain refinement) at higher strain rates and/or coarse grain sizes. These processes appear to occur continuously as a function of strain rates in a given material. Figure 17 shows microstructures in the fine grain material after large levels of strain. Grain growth is clearly visible at 5×10^{-5} s^{-1} and 2×10^{-4} s^{-1} and grain refinement at 10^{-2} s^{-1}. The extent of dynamic grain growth is greater than static, as shown in the interrupted data of Fig. 18. There does not appear to be a strong strain rate dependence of grain growth rate, although grain growth kinetics at 10^{-3} s^{-1} are somewhat more rapid. At 10^{-2} s^{-1}, there is no grain growth, simply grain deformation causing elongation along longitudinal and contraction along transverse directions. Since dynamic grain growth occurs at lower strain rates and dynamic recrystallization at higher strain rates, it is expected that grain size would remain unchanged at some intermediate strain rate. However, such a rate might be close to 10^{-2} s^{-1} and does not coincide with that of peak m or peak elongation

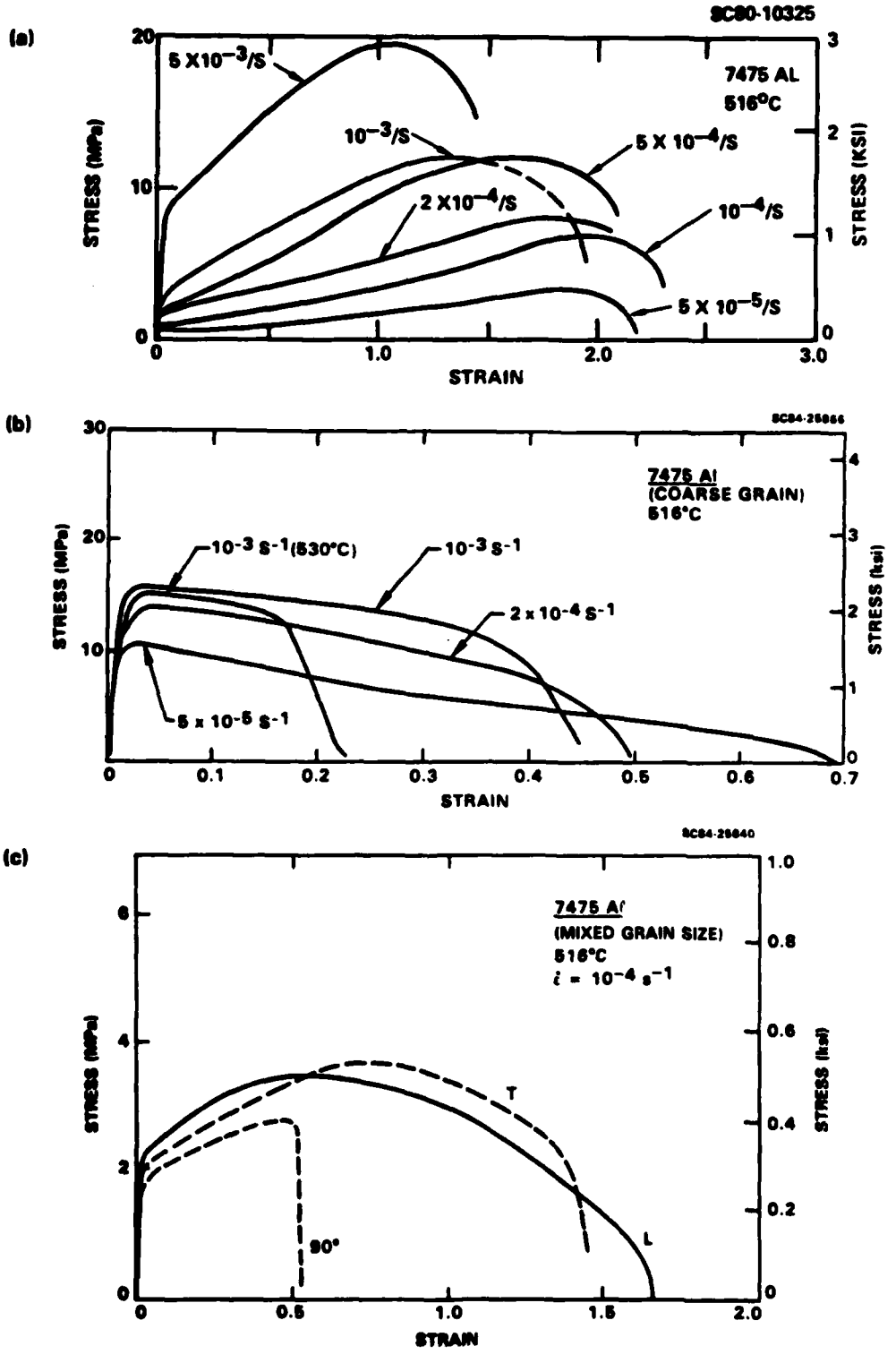

Fig. 16 Stress strain curves at various constant strain rates for (a) fine grain, (b) coarse grain, and (c) mixed grain size 7475 Al alloys.

SC83-22830

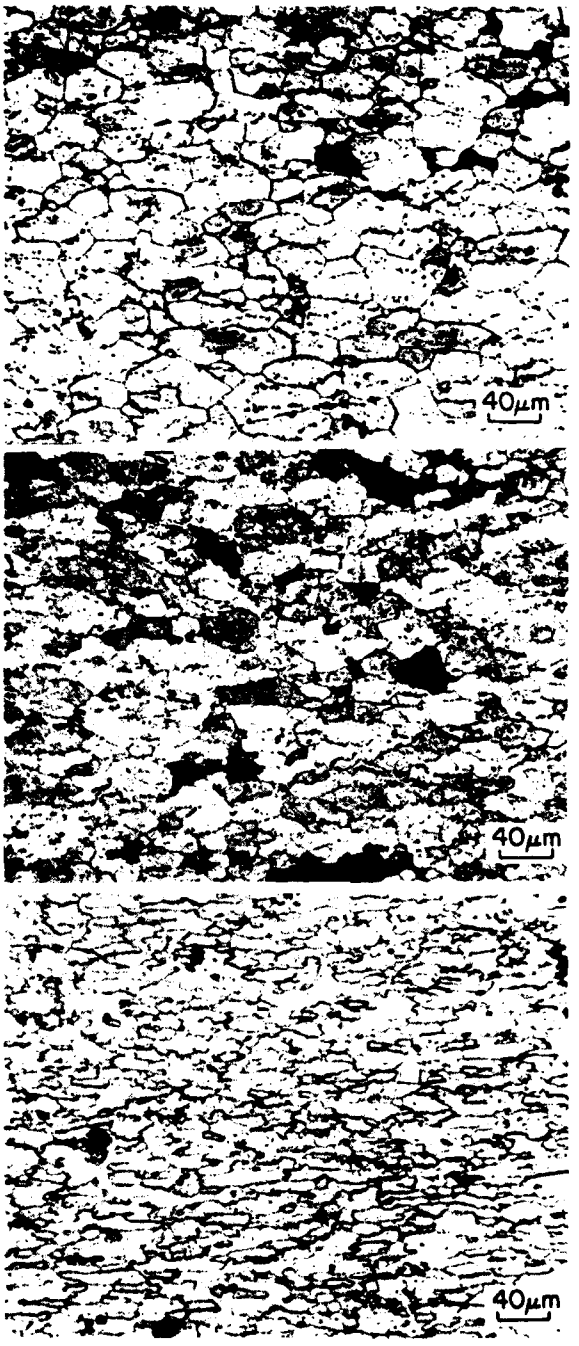

$\dot{\epsilon} = 5 \times 10^{-5}\ s^{-1}$
$\epsilon = 2.46$
$t = 763$ min

$\dot{\epsilon} = 2 \times 10^{-4}\ s^{-1}$
$\epsilon = 1.62$
$t = 171$ min

$\dot{\epsilon} = 10^{-2}\ s^{-1}$
$\epsilon = 1.02$
$t = 1.01$ min

Fig. 17 Microstructures near fracture of fine grain 7475 Al indicating extensive dynamic grain growth at low strain rates ($\leq 2 \times 10^{-4}\ s^{-1}$) and grain refinement at high strain rate ($10^{-2}\ s^{-1}$).

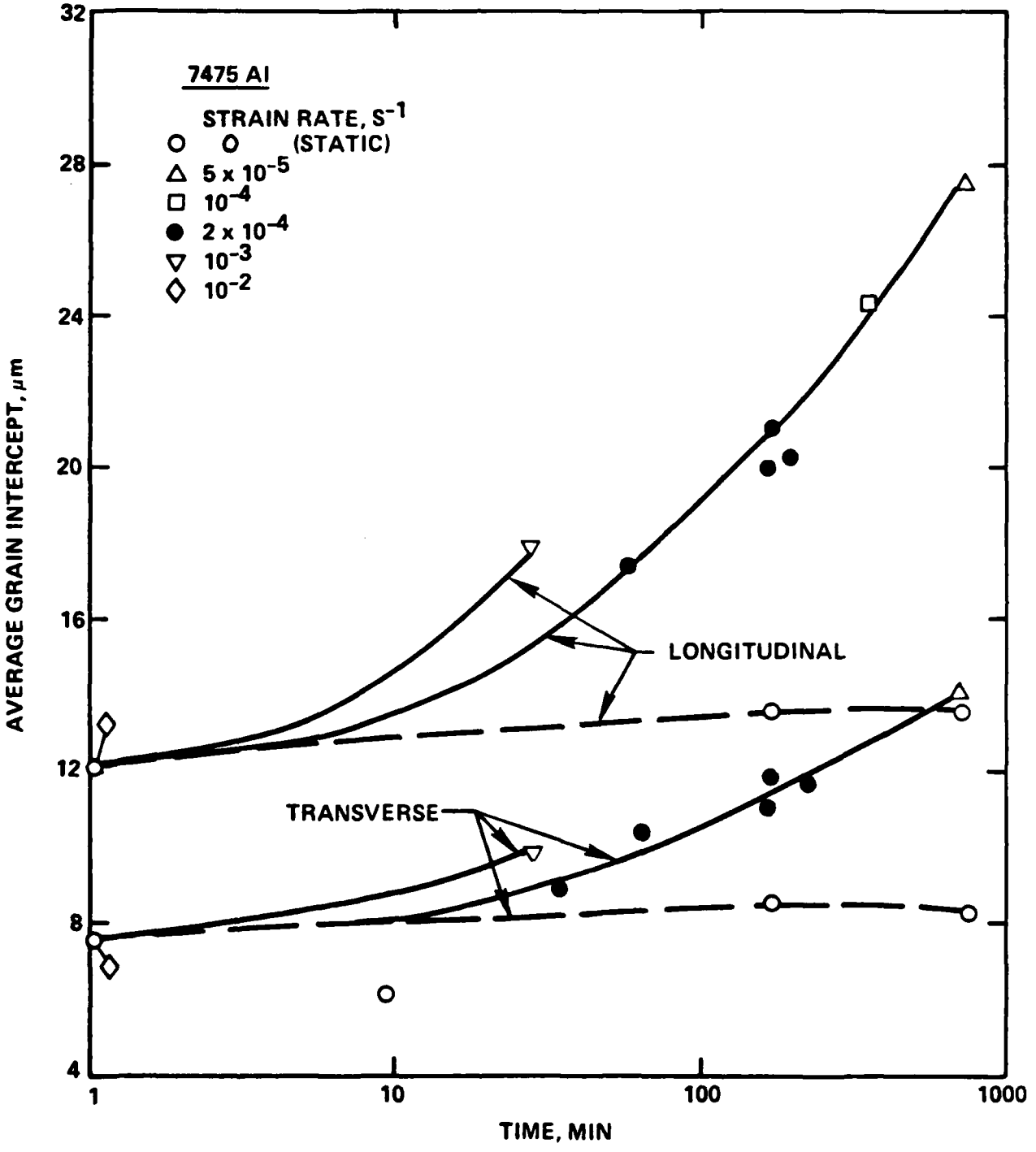

Fig. 18 Dynamic grain growth from interrupted tests at various constant strain rates compared with static grain growth for the fine grain 7475 Al.

($\sim 2 \times 10^{-4}$ s^{-1}). Thus, the high flow stability at 2×10^{-4} s^{-1} is not related to a fixed microstructure and might be partly associated with flow hardening from dynamic grain growth.

Figure 19 shows dynamic recrystallization effects in the coarse grain material after modest amounts of deformation. At all strain rates, larger grains were found fragmented into extremely fine grains. It appears that a critical plastic work for recrystallization is reached first in the larger grains, and subsequently in the smaller grains. Also shown in Fig. 19c is the microstructure after a high strain rate deformation at 10^{-1} s^{-1} (516°C) for the fine grain material. The grain elongation and slip bands (differing in orientation in the different grains) are clearly visible. Figure 20 provides further quantitative evidence of this effect. Plots of grain intercept distribution for the fine grain (Fig. 20a) and coarse grain (Fig. 20b) materials illustrate that during dynamic grain growth (fine grain material), the entire distribution curve (including the median size) shifts to a larger size with an increasing degree of deformation. The reverse is true during dynamic recrystallization (Fig. 20b). This type of information is vital to the development of the model for microstructural changes which is currently underway.

3.3.4.1 Development of a Mechanistic Model

The space is limited here to discuss the model development work in its entirety. However, a brief summary is presented, and the details may be found in the papers in preparation.[24-26] Based on the observations of slip during superplastic flow and other studies on dislocation structures,[27] the importance of dislocation processes during superplastic flow cannot be ignored. Recently, Arzt, Ashby and Verral[28] have considered grain boundary sliding occurring through the motion of grain boundary dislocations. However, the basic concept advanced here is that when crystallographic slip ossurs within the grains, dislocations continuously meet the grain boundaries, thereby changing the density of dislocations on the grain boundaries. This process

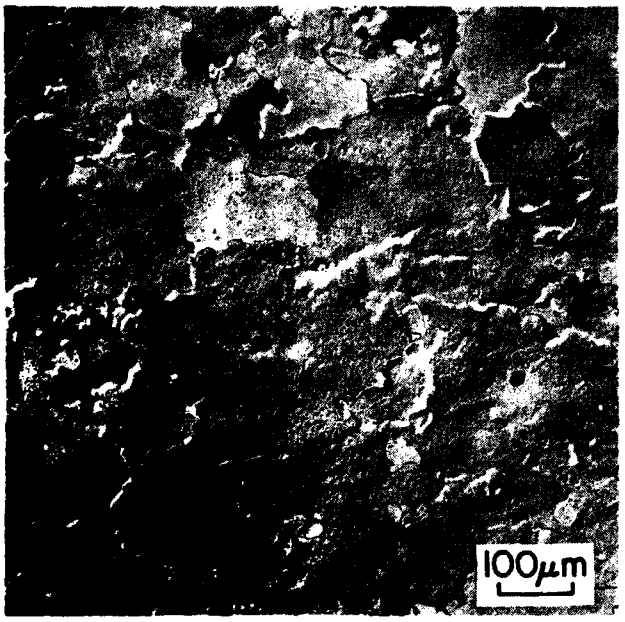

(a)

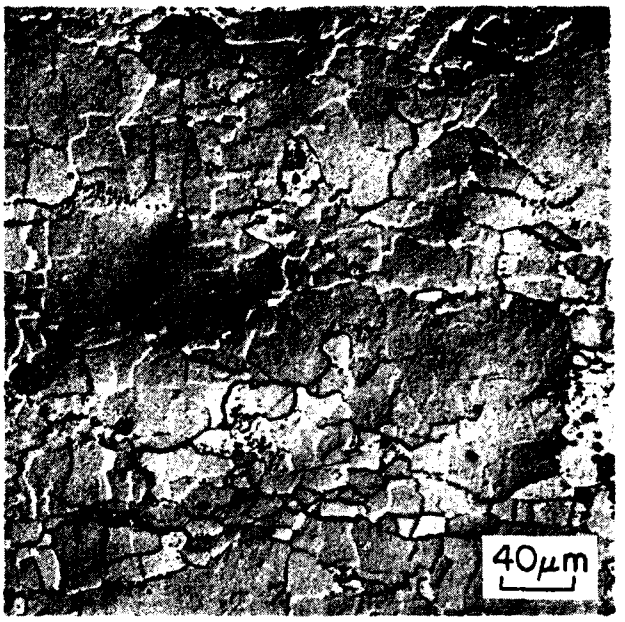

(b)

(c)

Fig. 19 Microstructure for coarse grain 7475 Al (a) zero strain, (b) $\varepsilon = 0.55$ at 516°C, $\dot{\varepsilon} = 2 \times 10^{-4}$ s^{-1}. Slip lines in fine grain 7475 Al deformed to $\varepsilon = 0.55$ at 516°C, $\dot{\varepsilon} = 10^{-1}$ s^{-1}.

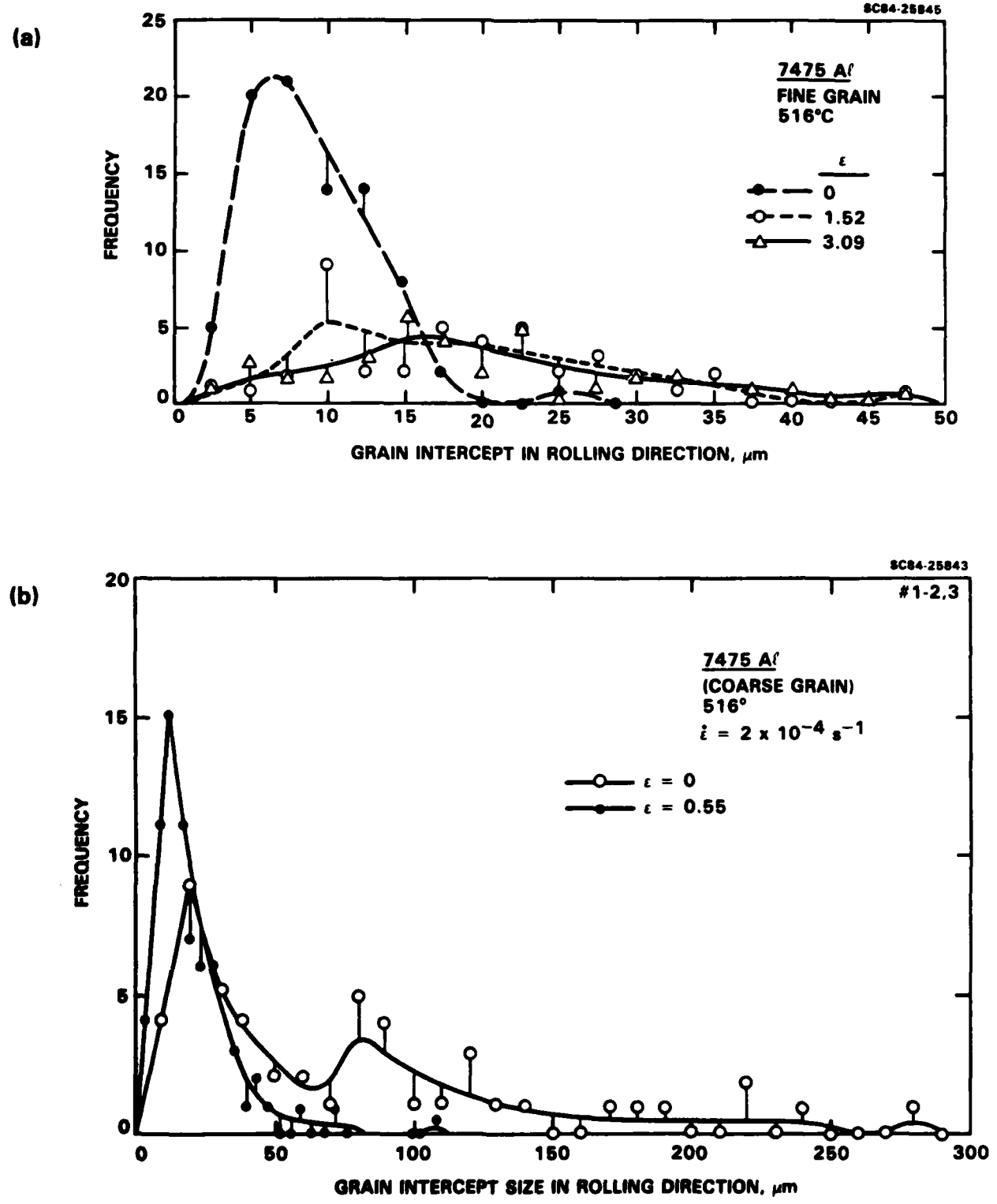

Fig. 20 Distribution of grain intercept along rolling direction after various strain levels for (a) fine grain, (b) coarse grain 7475 Al.

can cause an additional flux of matter along the grain boundaries, as well as change the misorientation about the boundaries. Thus, Coble diffusional creep rate (for grain boundary sliding) would be enhanced when the grains are undergoing deformation as opposed to being in an elastic state. Figure 21 shows how this would influence the flow behavior.

SC83-22825

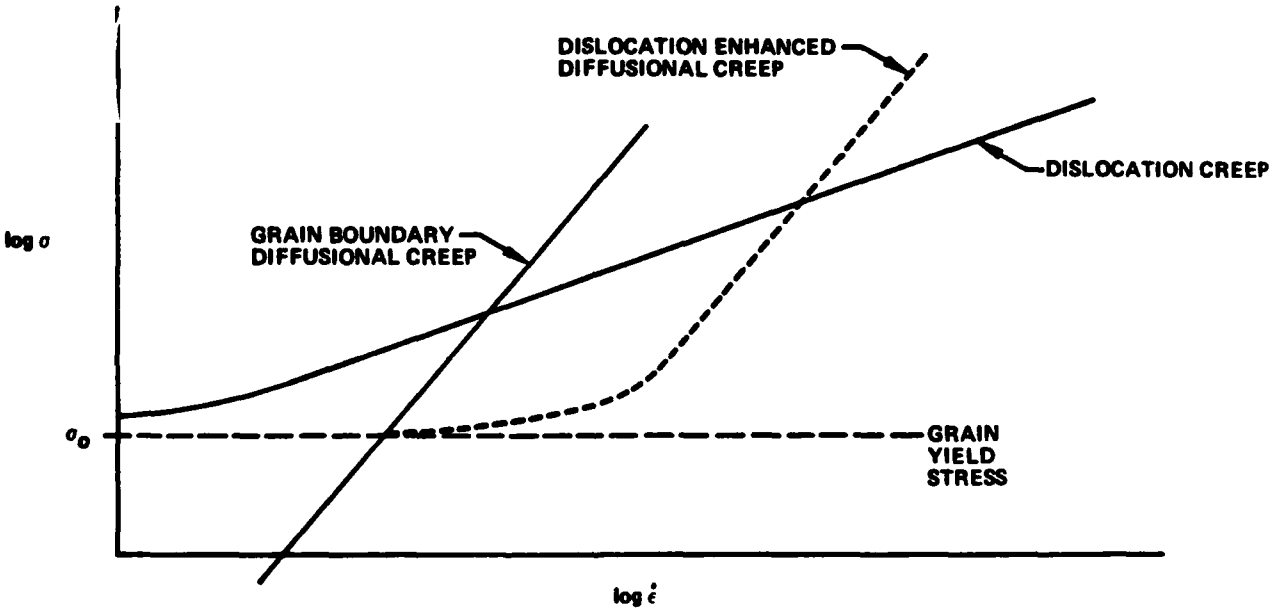

Fig. 21 Schematic illustration of σ-$\dot{\epsilon}$ curves for a model of superplasticity with dislocation enhanced diffusional creep.

If σ_0 is the average yield stress of grains below $\sigma = \sigma_0$, only diffusional creep would be expected. However, as $\sigma > \sigma_0$, grains would begin to deform, thereby accelerating diffusional creep (dotted curve). Eventually, a Newtonian viscous ($m = 1$) behavior would be approached at a higher strain rate. This combination thus explains the small threshold stress-like effects and high superplastic creep rates observed experimentally.

One of the key features of superplastic deformation is the slow

"strain induced hardening" observed up to very large strains. Since an increase in strain rate or a decrease in temperature increases $d\sigma/d\varepsilon$, it is clear that grain growth alone would not explain the hardening behavior, and dislocation structure development must be considered in the model. Thus, steady-state creep equations were replaced by hardening equations developed previously.[29] According to this, the incremental hardening equation is given by:

$$\dot{\sigma} = \left(\frac{nK^{1/n}}{\sigma^{1/n-1}}\right) \dot{\varepsilon}_g - \alpha(\sigma-\sigma_o)^r = E\,\dot{\varepsilon}_e \tag{1}$$

where $\dot{\sigma}$ = stress rate, $\dot{\varepsilon}_g$ = grain strain rate, $\dot{\varepsilon}_e$ = elastic strain rate, K = strength coefficient, n = strain hardening exponent, α = time constant for dynamic recovery, r = dynamic recovery exponent, and E = modulus of elasticity. The constraint equation for strain rate is

$$\dot{\varepsilon} = \dot{\varepsilon}_e + \dot{\varepsilon}_g + \dot{\varepsilon}_b \tag{2}$$

where $\dot{\varepsilon}$ = total strain rate, and $\dot{\varepsilon}_b$ = grain boundary diffusional strain rate, which is given by:

$$\dot{\varepsilon}_b = \left(\frac{A}{d^3}\right) \sigma \tag{3}$$

where $A = (42\,\Omega/kT)2D_B$, d = grain size, Ω = atomic volume and D_B = boundary diffusivity. The enhancement in diffusional creep has been given by the following exponential form:

$$A = A_o + (A^* - A_o)\,(1-e^{-\beta\dot{\varepsilon}_g}) \tag{4}$$

where A_o = initial value of A when $\dot{\varepsilon}_g = 0$, and A* = terminal value of A when $\dot{\varepsilon}_g \to \infty$, β = enhancement constant.

Addition of dynamic grain growth or dynamic recrystallization requires the use of appropriate kinetics or additional criterion, which are

being done currently. The outcome of this incremental deformation theory is that during dynamic grain growth, the mix of $\dot{\varepsilon}_g$ and $\dot{\varepsilon}_b$ continuously changes. The increase in $\dot{\varepsilon}_g$ (from very low values) with increasing strain is a very slow process, but one that leads to continuous hardening and a very slow approach to steady-state. This leads to the extreme flow stability in the superplastic range. Figure 22 shows how the balance of these strain rates can occur at steady-state for two different grain sizes. For a given applied strain rate, diffusional creep rates are rather high at the lower rates, but the coarser grain material undergoes more dislocation creep, thus increasing its tendency for dynamic recrystallization. The finer grain material can sustain a much higher degree of diffusional creep, even at the higher strain rates, thereby slowing down the development of dislocation creep and leading to extremely long transients. Further details of the model will be described in Refs. 24-26 and next year's annual report.

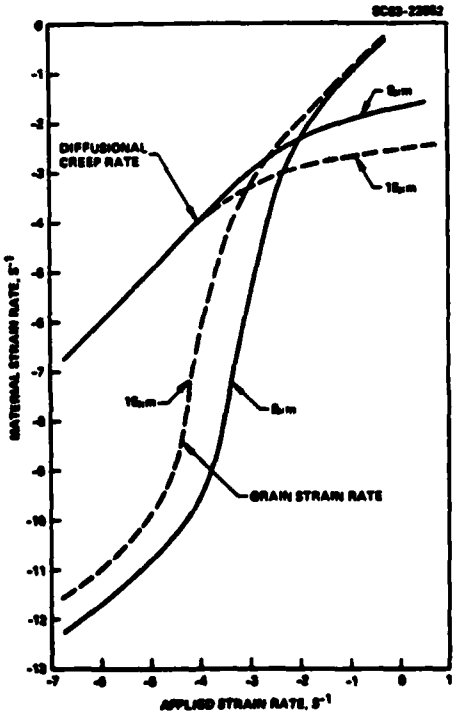

Fig. 22 Make-up of applied strain rate in terms of diffusional creep rate and grain strain rate for steady state.

4.0 REFERENCES

1. C.H. Hamilton et al, "Superplastic Forming of Titanium Structures," AFML-TR-75-62, April 1975.

2. "Preliminary Design and Material Allowables for SPF/DB Structures (BLATS)," Report No. NA-78-539-1, Rockwell International; Contract No. F-33615-77-C-3107, September 1978.

3. M.W. Mahoney and C.H. Hamilton, "Superplastic Aluminum Evaluation," AFWAL-TR-81-3051.

4. "Mechanical Behavior of Airframe Materials," Final Report, Contract No. F44620-76-C-0025, March 1980.

5. C.G. Rhodes, M.R. Mitchell and J.C. Chesnutt, "Fracture and Fatigue Characteristics in Ti Alloys," Final Report, SC5227.1FR, ONR Contract N00014-79-C-0567, June 1982.

6. "Development of Structural Titanium Alloy for Naval Application," Navy Contract N00024-80-C-5636.

7. G.R. Yoder, L.A. Cooley and T.W. Crooker, Met. Trans. 9A, 1413 (1978).

8. G.R. Yoder and D. Eylon, Met. Trans. 10A, 1808 (1979).

9. C.G. Rhodes, Electron Microscopy 1982, vol. 1, The Congress Organizing Committee, eds., Deutsche Gesellschaft fur Electronenmikroskipie, Frankfurt, 1982, pp. 663-64.

10. R.J. Bucci, "Development of a Proposed ASTM Test Method for Near Threshold Fatigue Crack Growth Rate Measurement," Fatigue Crack Growth Measurement and Data Analysis, ASTM STP 738, 5 (1981).

11. A.K. Ghosh and C.H. Hamilton, Met. Trans. A 10A, 699 (1979).

12. A.K. Ghosh and C.H. Hamilton, Proc. 5th Int. Conf. on Strength of Metals and Alloys, P. Haasen, ed., Aachen, p. 905, August 1979.

13. A.K. Ghosh, "Deformation of Polycrystals-Mechanisms and Microstructures," Proc. 2nd Int. Symp. on Met. and Mat. Sci., N. Hansen et al, eds., p. 277, September 1981.

14. M.F. Ashby and R.A. Verrall, Acta Metall. 21, 149 (1973).

15. F.R.N. Nabarro, Proc. Conf. Strength of Solids, Phys. Soc. of London, Cambridge, p. 75 (1948).

16. C. Herring, J. Appl. Phys. 21, 437 (1950).

17. R.L. Coble, J. Appl. Phys. 34, 1679 (1963).

18. A. Ball and M. Hutchinson, Met. Sci. J. 3, 1 (1969).

19. A.K. Mukherjee, Mat. Sci. Eng. 8, 83 (1971).

20. A.K. Ghosh and R. Raj, Acta Metall. 29, 607 (1981).

21. R. Raj and A.K. Ghosh, Acta Metall. 29, 283 (1981).

22. N.E. Paton and C.H. Hamilton, U.S. Patent 4,092,181, May 1978.

23. C.H. Hamilton, "Method for Superplastic Forming," U.S. Patent No. 4,354,369, October 1982.

24. A.K. Ghosh, "Slip-Enhanced Diffusional Creep and Superplasticity," in preparation.

25. A.K. Ghosh, "A Model for Static and Dynamic Grain Growth at High Homologous Temperatures," in preparation.

26. A.K. Ghosh, "A Mechanistic Model for Superplastic Flow in Single Phase Materials," in preparation.

27. C.G. Rhodes, unpublished work, Rockwell Science Center, 1982.

28. E. Arzt, M.F. Ashby and R.A. Verral, Acta Met. 31, (12), 1977 (1983).

29. A.K. Ghosh, Acta Met. 28, 1443 (1980).

5.0 PUBLICATIONS AND PRESENTATIONS

1. A.K. Ghosh, "Slip Enhanced Diffusion Creep and Superplasticity," in preparation, 1984.

2. A.K. Ghosh, "Invited Presentation at the 1983 Gordon Research Conference on Physical Metallurty, Plymouth, New Hampshire. This presentation was based on the above paper.

6.0 PERSONNEL

Personnel involved in Part I of this program are:

J.A. Wert, Program Manager
J.C. Chesnutt, Principal Investigator
C.G. Rhodes, Principal Investigator
R.A. Spurling
P.Q. Sauers
M. Calabrese

Personnel involved in Part II of this program are:

A.K. Ghosh, Principal Investigator
L.F. Nevarez
J.M. Curnow
G. Rivera.
M. Calabrese

7.0 COUPLING ACTIVITIES

1. The work on fatigue crack propagation on Ti-6Al-4V is highly relevant to the North American Aircraft Opertion, Rockwell International with regard to the B-1B bomber program. Ti-6Al-4V is used in the aircraft in applications requiring high resistance to fatigue crack propagation. The data regarding crack propagation behavior of material processed above the beta transus are of considerable interest to NAAO and are being furnished to their materials engineering staff.

2. Dr. J.C. Williams, Dean of Engineering, Carnegie-Mellon University has participated in substantial discussions of the program details, and of microstructure development and fatigue crack propagation of Ti alloys in general during a recent visit to the Science Center.

3. J.C. Chesnutt is currently co-authoring a paper with J.C. Williams and A.W. Thompson entitled, "Fatigue Crack Propagation in Ti Alloys", which will appear in the proceedings of an international conference, FATIGUE 84, to be held in Birmingham, England, September 3-7, 1984. Although the specific results of this program will not be reported, they will contribute to the authors' understanding of the effect of beta processing on fatigue crack propagation, and to discussion of the same in the paper.

4. Discussions with Prof. Rishi Raj of Cornell University several times during the last year are acknowledged. Prof. Raj will be a visiting scientist at the Science Center during April 1984, when joint work is contemplated.

5. Discussions with Prof. D. Wilkinson of McMaster University, Canada, June 1983.

6. Discussions with Prof. E. Nes, Norwegian Institute of Technology, Trondheim, Norway, June 1983.

7. Discussions with Prof. W.D. Nix, Stanford University, several times during 1983.

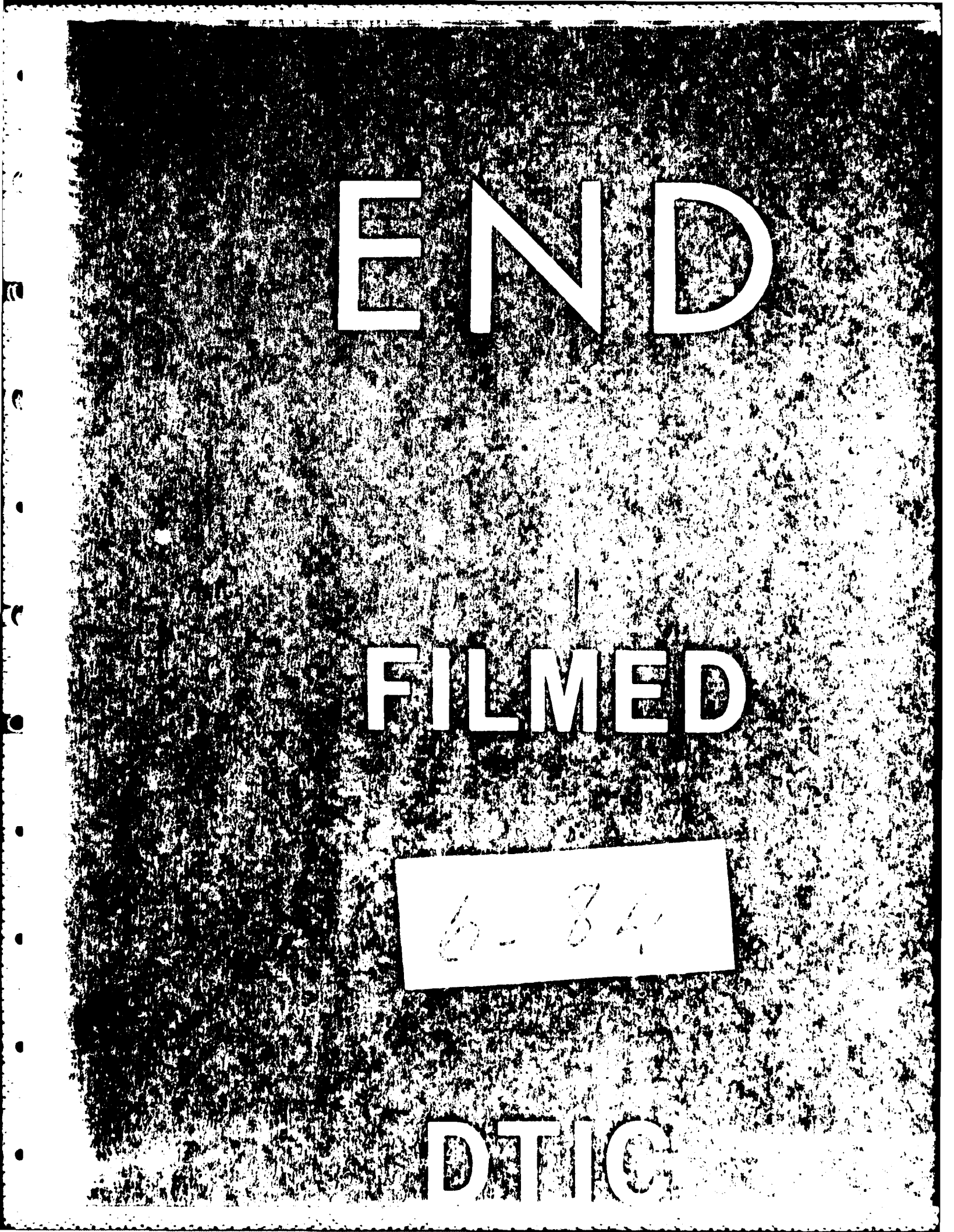
END
FILMED
6-84
DTIC